Progress In Electromagnetics Research Letters, Vol. 58, 97–103, 2016

High-Performance LPF Using Coupled C-Shape DGS and Radial Stub Resonators for Microwave Mixer

Abdelmounaim K. Belbachir*, Mohamed Boussouis, and Naima A. Touhami

Abstract—A high-performance microstrip low-pass filter (LPF) with low cutoff frequency, negligible passband insertion loss, very sharp transition band, and deep ultra-wide stopband is designed, fabricated and measured. The presented filter is realized using three types of resonators which are coupled C-shape defected ground structure (C-CDGS), mirrored series-resonant branch loaded by radial stub and high impedance line loaded by radial stub. A novel equivalent circuit model of the C-CDGS resonator is created, and its corresponding parameters are also extracted. The proposed filter is experimentally verified through the measured results which show good agreement with electromagnetic simulations.

1. INTRODUCTION

Low-pass filter (LPF) plays an important role in all frequency mixers [1]. The proposed LPF placed in output port of a microwave down-converter mixer must let pass just generated low-frequency mixing signal (around 1 GHz) and provide good rejection of high-frequency signals (around 11 and 12 GHz). Low cutoff frequency, negligible insertion loss, high selectivity, deeper wide stopband and compact size are the most important filtering characteristics of a required LPF for microwave mixer application.

Different techniques and structures have been reported in the recent researches to achieve a LPF with improved characteristics [2–14]. A stub-loaded coupled-line hairpin unit [2] and a folded stepped impedance open stub [3] are exploited to achieve a microstrip lowpass filter with high selectivity and wide stopband. An arrangement of several stepped impedance, radial stub and folded open stub resonators is proposed in [4] and [5] to realize a LPF with superior specifications such as sharp roll-off, wide stopband, good return loss and compact size, but this improvement has cost complicate structure. Another LPF design technique employing various forms of defected ground structures DGS [6] is presented in [7–14]. In [7], spurious harmonic of an even-order elliptic function LPF is eliminated by using conventional shaped DGS. In [8] and [9], stepped-impedance low-pass filter employing I-shaped and C-shaped thin slots DGS is presented to achieve ultra-wide stopband with 2 GHz cutoff frequency. In [10], a compact dual-planar electromagnetic bandgap microstrip low-pass filter configuration is investigated for achieving wide stopband. Low 3-dB cutoff frequency compact LPF using V-shaped DGS was proposed in [11]. The meandered slot in [12] provides a wideband resonator with low insertion loss and very sharp cutoff frequency response. In [13], a novel compact LPF with quarter-circle-shape DGS shows suppression levels approximately 20 dB from 4 GHz to more than 20 GHz. Moreover, the LPF in [14] has been designed by employing a novel DGS pattern with two attenuation poles to obtain a sharp selectivity and a very wide rejection bandwidth with the cost of large size. However, these filters' performances do not completely achieve all the filtering characteristics of a required LPF for the down-converter mixer.

In this work, a LPF with all excellent filtering characteristics for a microwave mixer is achieved. It is based on microstrip radial stubs and coupled DGS resonators. The design takes advantage of using both sides of the substrate, so a novel equivalent circuit model of the coupled DGS resonator is developed. Experimental justification of the simulation is also provided.

Received 1 September 2015, Accepted 5 January 2016, Scheduled 24 January 2016
* Corresponding author: Abdelmounaim Kchairi Belbachir (belbachir.kochairi@gmail.com).
The authors are with the Faculty of Sciences, University Abdelmalek Essaidi, Tetouan, Morocco.

2. DESIGN PROCEDURE

Figure 1 shows the geometry structure of the proposed LPF Resonator 1 which is composed of two coupled C-shape DGS cells etched in ground plan. Resonator 2 is composed of mirrored series-resonant branch loaded by radial stub. Resonator 3 is made of high impedance microstrip line loaded by radial stub. It should be noted that the circuit is designed on an FR4 substrate having a thickness of $h = 0.762\,\mathrm{mm}$, permittivity of $\varepsilon_r = 4.5$, and dielectric loss tangent of $\tan\delta = 0.021$. The EM simulation is obtained by using CST Microwave Studio tool.

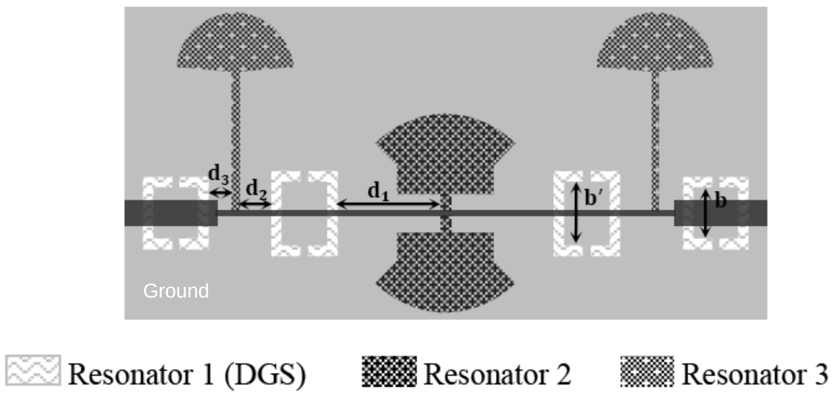

Figure 1. Layout of resonators used in the LPF design. Grey zones represent the metallization of microstrip: the dark shade denotes the top layer, while the light shade represents the ground.

To simplify the design theory of the proposed filter, the following steps are used. The first step is to realize the equivalent circuit model of resonator 1. The second step is to design and analyze microstrip resonators 2 and 3. The third step is to combine the three resonators correctly to implement the proposed LPF. The final step is to fabricate a prototype and measure the performances.

2.1. Resonator 1 Design and Circuit Modeling

Figure 2(a) shows the configuration of a C-shape DGS (CDGS) unit etched in the ground plan layer under a transmission line. The parameters (in millimeters) are: $a = 1.1$, $b = 3$ and $w = 0.6$. The calculated width w_0 of the microstrip transmission line is 1.39 so as to attain $Z_0 = 50\,\Omega$ of characteristic impedance. The microstrip line coupled to the CDGS can be considered effectively as a short-circuited $\lambda/4$ line and acts as a parallel LC resonance circuit near the resonance frequency. According to [6], CDGS can be represented by the parallel LC model of Fig. 2(b). It can be observed from EM simulation in Fig. 2(c) that the resonance frequency f_0 is around 17.5 GHz and the 3-dB cutoff frequency f_c around 13.45 GHz.

The parallel LC resonator of the equivalent circuit is given by [6].

$$C_R = \frac{\omega_c}{Z_0 g_1} \cdot \frac{1}{\omega_0^2 - \omega_c^2} \tag{1}$$

$$L_R = 1/4\pi^2 f_0^2 C_R \tag{2}$$

where ω_0 is the resonance angular frequency, ω_c the 3-dB cutoff angular frequency, g_1 the Butterworth one-pole prototype low-pass filter element, and Z_0 the characteristic impedance of the microstrip line. The circuit parameters extracted from the EM simulation are $L_R = 0.485\,\mathrm{nH}$ and $C_R = 0.17\,\mathrm{pF}$.

In order to design a filter with improved bandstop, two CDGS resonators which have equal size and inverse direction are placed close together along with the transmission line as shown in Fig. 3(a). The coupling intensity between the CDGS resonators depends on the separation distance s. The coupling coefficient can be calculated from the well-known following equation.

$$k = \left| \frac{f_1^2 - f_2^2}{f_1^2 + f_2^2} \right| \tag{3}$$

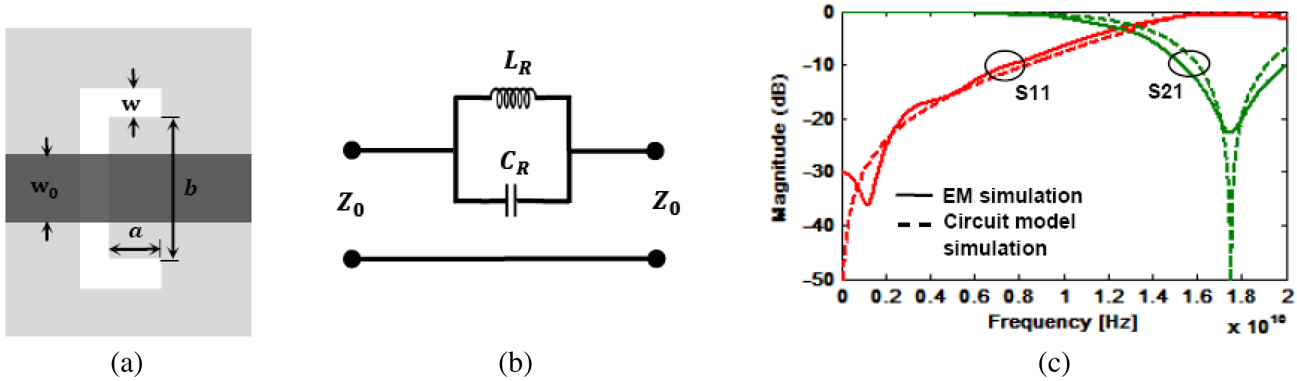

Figure 2. C-shape DGS unit, (a) structure, (b) equivalent circuit model, (c) circuit and EM simulations.

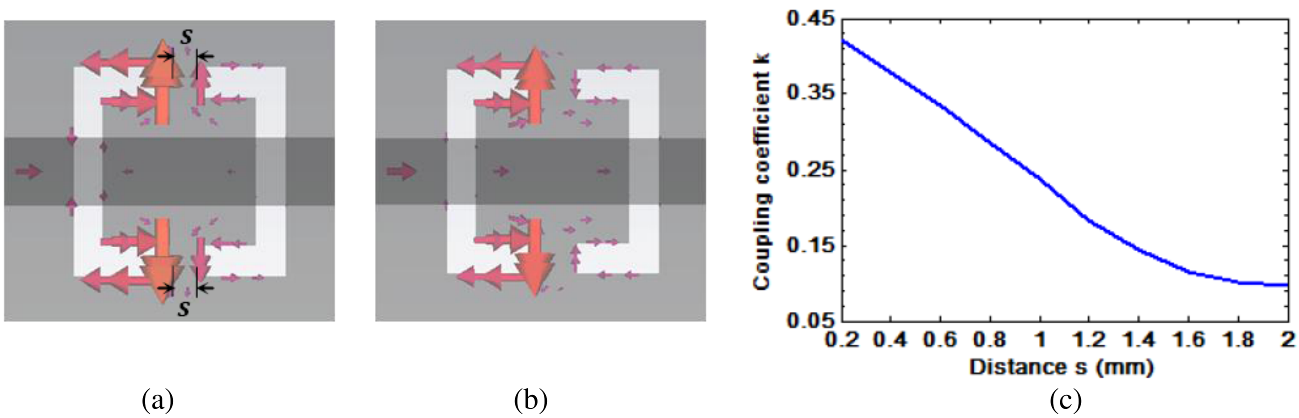

Figure 3. Ground current pattern of inductive coupling in coupled CDGS resonators for (a) f_1 frequency and (b) f_2 frequency, (c) coupling coefficient k as a function of distance s.

where f_1 and f_2 are two resonance frequencies exhibited by the two CDGS resonators due to the coupling effect.

To identify the nature of the coupling between CDGS resonators, the ground current orientation in the two coupled CDGS resonators at frequencies f_1 and f_2 is investigated. As seen from Fig. 3(a), for the first frequency ($f_1 = 13.1\,\text{GHz}$ in the case $s = 0.4\,\text{mm}$), if current circulation of first CDGS is clockwise, then the current circulation of second CDGS will be anti-clockwise and vice-versa. For the second frequency ($f_2 = 19.65\,\text{GHz}$) as in Fig. 3(b), the current circulation in both resonators takes either anti-clockwise or clockwise orientation simultaneously. As a result, the coupled CDGS resonators exhibit inductive coupling with negative mutual inductance effect [15]

$$L_m = -kL_R \tag{4}$$

Using Equations (3) and (4), the coupling coefficient and mutual inductance in the case $s = 0.4\,\text{mm}$ are $k = 0.3781$ and $L_m = -0.1834\,\text{nH}$, respectively.

The effect of distance s on the coupling coefficient k is illustrated in Fig. 3(c). It is observed that an increase in s results in a decrease in k. As the distance between the two CDGS resonators is increased, fewer fields couple between the resonators.

Figure 4(a) represents the simple equivalent LC circuit used to develop the novel detailed equivalent circuit shown in Fig. 4(b) for the magnetically coupled CDGS resonators. The negative mutual inductance L_m is multiplied with 2 because there are two coupling gaps between CDGS resonators. The negative coupling effect increases the stored flux in the single resonator circuit, so that the resonant frequency f_0 is shifted down to 13.4 GHz [16].

As shown in Fig. 4(c), the attenuation pole f_0, due to the negative coupling effect, greatly improves

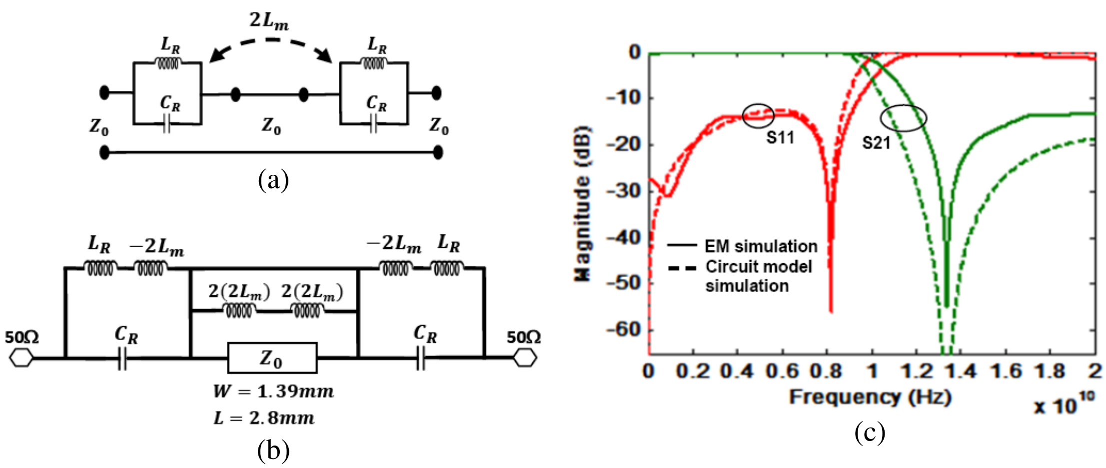

Figure 4. Coupled CDGS filter, (a) the simple equivalent circuit, (b) the novel detailed equivalent circuit model for the magnetically coupled CDGS resonators, (c) fall wave electromagnetic simulation compared with circuit model simulation (in case $s = 0.4\,\mathrm{mm}$).

the stopband rejection, i.e., a broad-stopband ($-13.8\,\mathrm{dB}$) from 12 GHz to more than 20 GHz is achieved. It can be observed that there is a very good similarity between circuit simulation and EM-simulation, which verifies the success of the proposed novel model.

2.2. Resonators 2 and 3 Design and Analysis

A second filter with mirrored series-resonant branch loaded by radial stub is designed. First, a conventional compact three-order microstrip low-pass filter with open-circuited stub is designed (Fig. 5(1) and Fig. 5(a-1)), where the high characteristic impedance lines ($w_1 = 0.3\,\mathrm{mm}$, $l_1 = 10.25\,\mathrm{mm}$) act as series inductors and the low impedance open-circuited stub ($w_2 = 5.5\,\mathrm{mm}$, $l_2 = 1.8\,\mathrm{mm}$) as shunt capacitor [17]. In order to excite a transmission zero (Fig. 5(a-2)), two apertures with the length of

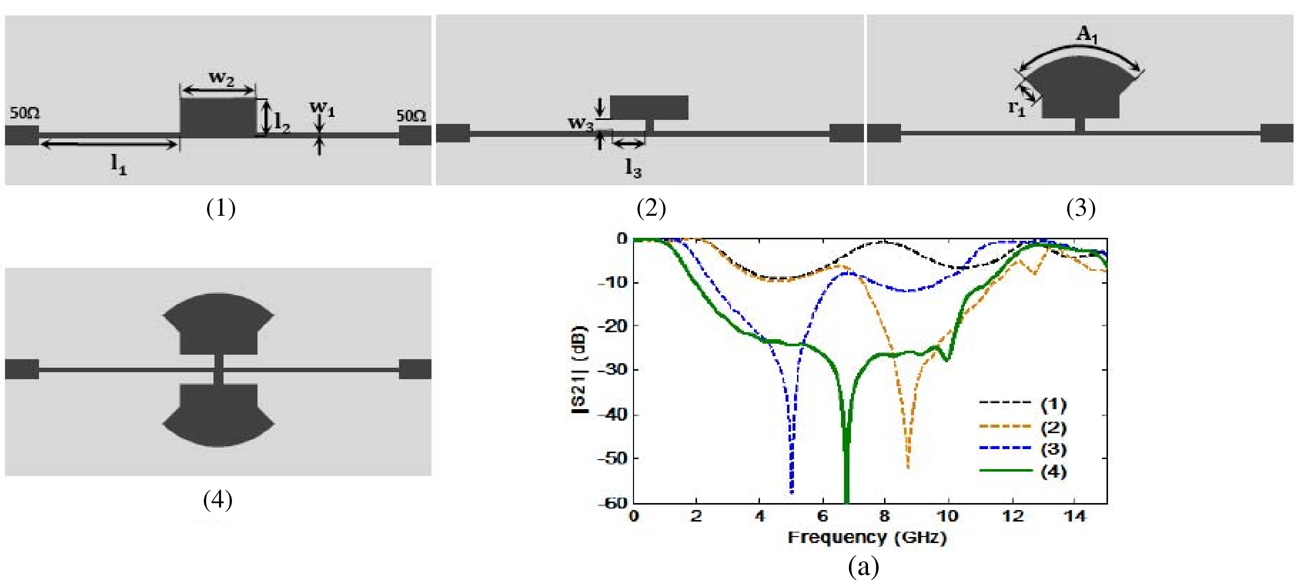

Figure 5. Mirrored series-resonant branch loaded by radial stub resonator design process and simulations. (1) 3-pole LPF using open-circuited stub, (2) series-resonant branch, (3) series-resonant branch loaded by radial stub, and (4) mirrored structure, (a) S_{21} simulations.

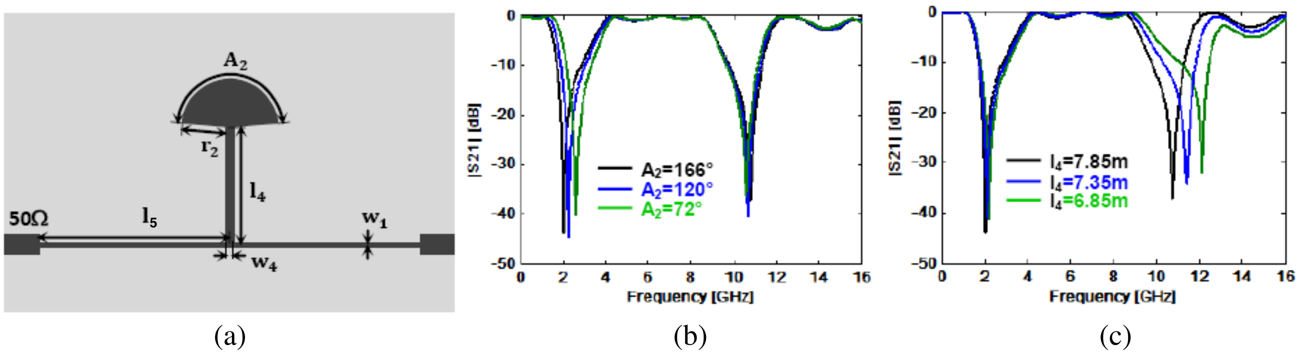

Figure 6. High impedance lines loaded by radial stub resonator, (a) structure, (b) transfer characteristics for different A_2 ($l_4 = 7.85$ mm), (c) transfer characteristics for different l_4 ($A_2 = 166°$).

$l_3 = 2.45$ mm and width of $w_3 = 0.9$ mm are etched inside the open-circuit as shown in Fig. 5(2). A series-resonant branch that shorts out transmission at its resonant frequency is obtained [18]. To improve the selectivity, a radial stub ($A_1 = 91°$, $r_1 = 1.8$ mm) is added at the terminal of the series-resonant branch to move the transmission zero toward 3-dB cutoff frequency (Fig. 5(3) and Fig. 5(a-3)). Finally, a mirrored structure of the series-resonant branch loaded by radial stub is added to achieve a wide stopband (Figs. 5(4) and (a-4)).

By using the mirrored series-resonant branch loaded by radial stub, a filter with low 3-dB cutoff frequency at 1.4 GHz and wide rejection area starting from 3 to more than 10 GHz is achieved. However, both the stopband and the sharpness still need improvement.

As can be seen from Fig. 6(a), the third resonator consists of high impedance lines loaded by radial stub. The dimensions are as follows: $l_5 = 13$ mm, $w_1 = 0.3$ mm, $l_4 = 7.85$ mm, $w_4 = 0.4$ mm, $A_2 = 166°$, $r_2 = 3.1$ mm.

Figures 6(b) and (c) illustrate the frequency response of the proposed resonator as the functions of angle A_2 and length l_4, respectively. It can be seen from the results that the resonator exhibits two deep transmission zeros that are affected separately by A_2 and l_4. When l_4 is fixed and A_2 decreased, the low transmission zero location moves up to upper frequencies. On the other hand, when A_2 is fixed and l_4 decreased, the high transmission zero location moves up. So, the locations of two transmission zeros can be easily adjusted by changing only the parameters A_2 and l_4 in the proposed resonator.

2.3. High-Performances LPF Implementation and Measurement

Based on the proposed three resonators, a high-performance low-pass filter has been designed (Fig. 1). The resonators are properly combined in both sides of the substrate. The distance between resonators is optimized using EM simulation ($d_1 = 5.8$ mm, $d_2 = 1.8$ mm, $d_3 = 1.3$ mm). Firstly, two wide stopbands are achieved by adding four cascaded resonator 1 units ($b' = 3.6$ mm) to resonators 2. Secondly, selectivity and stopband are improved by connecting two units of resonator 3 at both sides of resonator 2. In fact, the low transmission zero of resonator 3 causes an attenuation poles close to the cutoff frequency 1.4 GHz of resonator 2 which leads to obtaining sharp transition band while the high transmission zero of resonator 3 gather together the two stopbands of resonators 1 and 2. Consequently, ultra-wide stopband is obtained.

Figure 7 shows a photograph of the fabricated LPF. Its S-parameters are measured by using Rohde and Schwarz ZVB 20 vector network analyzer. The electromagnetic simulations and measured results, which are in good agreement, are shown in Fig. 8. The measured radiation losses around 10 and 16 GHz can be ignored because they are less than 10 dB. The results indicate that the filter presents numerous remarkable characteristics such as small 3-dB cutoff frequency of 1.56 GHz, very sharp transition band of 115.6 dB/GHz, negligible insertion loss lower than 0.32 dB, low return loss inferior to −15.7 dB and ultra-wide stopband from 1.75 GHz to more than 20 GHz of at least 21 dB suppression levels and has also a relatively compact size of only $0.37\lambda_g \times 0.182\lambda_g$. For comparison, Table 1 summarizes the performance of the proposed LPF and other related LPFs.

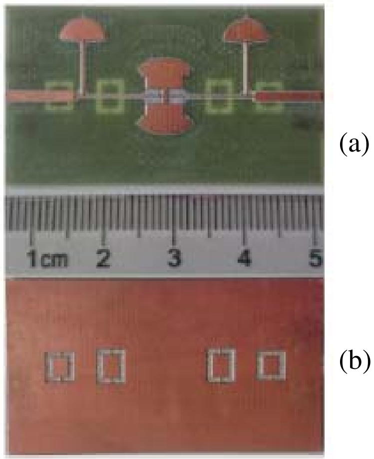

Figure 7. Photographic views of proposed LPF, (a) top view, (b) bottom view.

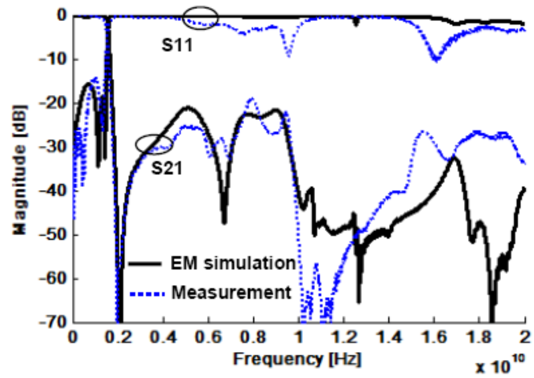

Figure 8. EM simulation and measurement results.

Table 1. Summaries and comparisons.

Ref.	Substrate dielectric constant/ Height (mm)	Insertion loss (dB)	Cutoff frequency (GHz)	transition band (dB/GHz)	Stopband (GHz@dB)	Normalized circuit size ($\lambda_g \times \lambda_g$)
[3]	3.38/0.508	0.37	2.28	121	(2.42 to 14.9 @ 20)	0.271 × 0.15
[4]	3.38/0.508	0.4	1.796	140	(2.02 to 15.14 @ 25)	0.247 × 0.107
[5]	2.2/0.7874	0.164	2.37	528.57	(2.4 to 16 @ 13.2)	0.324 × 0.109
[11]	3.38/1.524		1.688	gradual	(2.22 to 7.12 @ 20)	0.204 × 0.193
[12]	4.4/0.8	0.7	> 2.5	51	(2.9 to 12 @ 20)	0.342 × 0.189
[13]	3.38/0.813	0.1	2.95	gradual	(4 to 20 @ 20)	0.426 × 0.266
[14]	2.2/0.508		3.25	56.25	(3.75 to 30 @ 30)	1.062 × 0.128
This work	4.5/0.762	0.32	1.56	115.6	(1.75 to 20 @ 21)	0.37 × 0.182

3. CONCLUSION

In this paper, a high-performances low-pass filter using coupled C-shape DGS and radial stub resonators is designed, fabricated and measured. To describe the coupled CDGS resonator, a novel equivalent circuit model is given in detail. The design process of the mirrored radial stub resonator configuration is described step by step. By utilizing correct arrangement of resonators, a filter with numerous excellent performances such as low cutoff frequency, negligible passband insertion loss, excellent skirt selectivity, and deep ultra-wide stopband is obtained. With these advantages, the proposed filter may have wide applications in the design of microwave mixers.

ACKNOWLEDGMENT

The authors would like to thank the Department of Communication Engineering, University of Cantabria.

REFERENCES

1. Maas, S. A., *Microwave Mixers*, 2nd edition, Artech House, London, 1993.
2. Velidi, V. K. and S. Sanyal, "Sharp roll-off lowpass filter with wide stopband using stub-loaded coupled-line hairpin unit," *IEEE Microwave and Wireless Components Letters*, Vol. 21, No. 6, 301–303, May 2011.
3. Makki, S. V., et al., "Sharp response microstrip LPF using folded stepped impedance open stubs," *Radioengineering*, Vol. 22, No. 1, 328–332, April 2013.
4. Mousavi, S. M. H., et al., "Design of high performance LPF with excellent return loss using stepped impedance and radial resonators," *International Journal of Engineering & Technology Sciences (IJETS)*, Vol. 03, No. 1, 32–44, January 2015.
5. Hayati, M. and A. Sheikhi, "Microstrip lowpass filter with very sharp transition band and wide stopband," *ETRI Journal*, Vol. 33, No. 6, 981–984, December 2011.
6. Weng, L. H., Y.-C. Guo, X.-W. Shi, and X.-Q. Chen, "An overview on defected ground structure," *Progress In Electromagnetics Research B*, Vol. 7, 173–189, 2008.
7. Banerji, A., "Design of a wide stopband harmonic suppressed microstrip low pass planar filter using defected ground structure," *International Journal on Electrical Engineering and Informatics*, Vol. 4, No. 1, 134–147, March 2012.
8. Kushwah, M. and D. Thakur, "Design of compact lowpass filter with wide stopband using I-shape," *International Journal of Engineering Sciences & Research Technology*, Vol. 3, No. 3, 1603–1605, March 2014.
9. Wu, J.-Y., Y.-H. Tseng, and W.-H. Tu, "Design of compact lowpass filter with ultra-wide stopband using thin slots," *Progress In Electromagnetics Research C*, Vol. 31, 137–151, 2012.
10. Zhang, H., Z. Xu, Y. Lin, and R. Wu, "A novel DP-EBG structure for low-pass filter of wide stopband," *PIERS Proceedings*, 1477–1480, Guangzhou, China, August 25–28, 2014.
11. Shaheen, M., et al., "Compact LPF design with low cutoff frequency using V-shaped DGS structure," *International Journal of Electronics and Communication Engineering & Technology (IJECET)*, Vol. 6, No. 1, 1–7, January 2015.
12. Wang, C.-J. and T. H. Lin, "A multi-band meandered slotted-ground plane resonator and its application of lowpass filter," *Progress In Electromagnetics Research*, Vol. 120, 249–262, 2011.
13. Challal, M., A. Boutejdar, et al., "Compact microstrip low-pass filter design with ultra-wide reject band using a novel quarter-circle DGS shape," *ACES Journal*, Vol. 27, No. 10, 808–815, October 2012.
14. Li, Y., H.-C. Yang, and S.-Q. Xiao, "Lowpass filter with wide stopband and sharp skirt using novel defected ground structure," *Progress In Electromagnetics Research Letters*, Vol. 41, 185–191, 2013.
15. Jung, S., Y.-K. Lim, and H.-Y. Lee, "A coupled-defected ground structure lowpass filter using inductive coupling for improved attenuation," *Microw. and Opt. Technol. Lett.*, Vol. 50, No. 6, 1541–1543, June 2008.
16. Hong, J.-S., and M. J. Lancaster, "Couplings of microstrip square open-loop resonators for cross-coupled planar microwave filters," *IEEE Transactions on Microwave Theory and Techniques*, Vol. 44, No. 12, December 1996.
17. Belbachir Kchairi, A., et al., "A novel compact lowpass filter using open-rectangle DGS technology for microwave mixers," *International Journal of Microwave and Optical Technology*, Vol. 10, No. 6, November 2015.
18. Hong, J.-S. and M. J. Lancaster, *Microstrip Filters for RF/Microwave Applications*, John Wiley & Sons, New York, 2001.